A Semi-Hidden Markov Modeling of a Low Complexity FSK-OOK In-House PLC and VLC Integration

A.D. Familua*, A.R. Ndjiongue†, K. Ogunyanda†, L. Cheng*, H.C. Ferreira† and T.G. Swart†
*School of Electrical and Information Engineering,
University of the Witwatersrand, Private Bag 3, Wits. 2050, Johannesburg, South Africa.
Email: Ayokunle.Familua@students.wits.ac.za
†Department of Electrical and Electronic Engineering Science,
University of Johannesburg, Auckland Park, 2006, South Africa.
Email: ogunyanda@gmail.com

***Abstract*—The integration of power line communication (PLC) and visible light communication (VLC) is increasingly receiving a lot of research interest with the advent of (IEEE 1901, ITUT G.9960/61) and IEEE 802.15.7 standards for PLC and VLC respectively. In particular, there is an underlying gain that could be achieved by leveraging the existing ubiquitous power line network infrastructure to render connectivity, while we also exploit the illumination system of power-saving Light Emitting Diodes (LEDs) for wireless data communication. The ubiquitous nature of these two systems makes us belief that VLC can offer a good complementary wireless data transmission technology to the existing In-House PLC in a similar manner broad-band Ethernet connections enjoys the support of Wi-Fi. This paper thus reports an implementation of a low complexity FSK-OOK In-House PLC and VLC Integration, as well as it's Second-Order Semi-Markov Model. The resulting statistical models facilitates the design and evaluation of forward error correcting codes to mitigate burst error occurrences, as well as optimizing the performance of the overall system.**

***Index Terms*—FSK-OOK Modulation, LEDs, Mamba Narrow-band Powerline Communication Shield, Power Line Communications, Visible light communications**

I. Introduction

PLC wireline technology affords us the luxury of harnessing the existing ubiquitous power line network for data transmission. This technology offers a wide variety of services such as home internetworking and automation, as well as providing a medium for internet connectivity, hence solving the last mile problem. On the other hand, VLC technology is a short-range optical wireless communication (OWC) technology that utilizes the visible light spectrum for data transmission. It exploits visible light sources such as White LEDs for both illumination and communication purposes. The ubiquitous nature and advantages these two medium of communication possess can be harnessed, such that VLC is made to offer a good complementary wireless data communication to the existing ubiquitous In-House PLC channel. Therefore, this paper thus reports an implementation of a low cost, low complexity FSK-OOK In-House PLC and VLC Integration utilizing Mamba power line communication shield. A First and Second-Order Semi-Markov Modeling of the burst error that occurs on the overall system is also carried out, based on the need to mitigate these burst errors. The resulting statistical Markov models furnishes us with information about the distribution of the burst errors, which can be used to facilitate the design and evaluation of forward error correcting codes for burst error mitigation, as well as useful in optimizing the overall system performance.

The rest of the paper is organized as follows. Section II discusses background details on following: Visible light communication, the implementation of the VLC module, a concise description of the low cost PLC module used, the Semi-Hidden Markov model, a Second-Order model and the algorithm for the parameterization of the model. Section III presents and discusses the experimental setup showing how the PLC and VLC modules are integrated. The Semi-Hidden Markov model results are in Section IV. Section V concludes the paper.

II. Background

A. Visible Light Communication

White LEDs are gradually taking over a great deal of our everyday life. Visible light communication is thus defined as a short-range OWC (optical wireless communication) employing visible light source (e.g White LEDs) for both illumination and high speed wireless data transmission purposes [1]. An attractive aspect of these LED devices is the fact that apart from its original use for lighting purposes, it can also be used for data communication purposes. Data transmission at high speed is fast becoming part of what is playing a major role in our day-to-day life in this modern century. Availability of multimedia data/information is envisioned to be within our reach at different places at any given time. A key element in the realization and achievement of this feat is the wireless access networks (WANs).

Nevertheless, there is scarcity of frequency ranges in the radio frequency spectrum where practicable spatial coverage could be achieved, hence it poses a limiting factor. Consequently,

other wireless communication means needed to be explored. Visible light communication (VLC) utilizing solid-state visible light sources such as white LEDs offers a possible alternative with the following advantages [2]: Possible integration with existing power line network, Visible light transmitters and receivers are inexpensive, Free from external intruders and eavesdroppers as the light-waves are only concentrated in a particular region and can not penetrate opaque objects and Radiations from the visible light sources are not harmful to human also free from radio frequency interference, hence, its use in air planes is safe. A comprehensive literature on VLC systems, it's underlying fundamentals and its integration with PLC systems can be found in the following literatures: [2]–[4]

B. Visible Light Communication System Architecture

The VLC transmission system architecture is depicted in Figure 1 as follows.

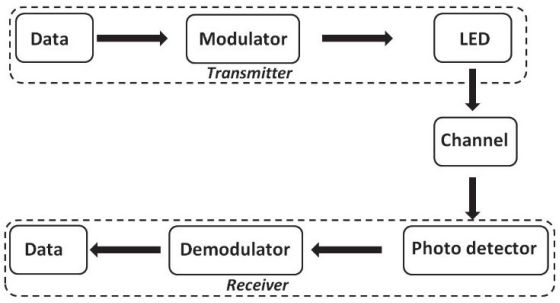

Fig. 1. Visible light communication system architecture

A concise discussion of the major building block of the VLC system (the transmitter, the channel and the receiver) are presented as follows. *The transmitter*: The VLC transmitter has the signal conditioning module, the modulation module and the LED. The combination of the LED and a modulation scheme depends on two main factors: the application of the communication system and the utilization of the lighting system. Two important constraints are to be met by the transmitter: Firstly, the optical power must remain constant during data transmission and, secondly, the communication throughput must be optimized. *The channel*: In VLC, the channel is represented by the air interface between the transmitter and the receiver. The channel is influenced by different sources of impairment, such as noise and interference sources, which must be distinguished from each other. The most important noise in the VLC channel is the shot noise modeled using poisson distribution.

The receiver: The main element in the VLC receiver is the photo-detector used to collect the light radiation. Two main types of photo-detectors are used in VLC receivers: the photo-diode and the phototransistors. Components such as concentrator, optical filter, amplifier and equalizer are added to the photo-detector to build a complete VLC receiver. In VLC, the transmission is governed by the following equation:

$$r(t) = h(t)s(t) + n(t)$$

Where $r(t)$, $h(t)$, $s(t)$ and $n(t)$ are the received signal, the channel impulse response, the transmitted signal and the channel noise respectively.

The Modulator (On-off keying modulation technique): Different modulation techniques are available to be used in VLC. Most of them are dedicated for specified situations. One distinguishes the variable pulse position modulation (VPPM), which is a variance of PPM, the colour shift keying (CSK) and the on-off keying (OOK) to mention only a few [5], [6]. By definition, IEEE 802.15.7 is the standard that gives rules and regulation for VLC [2]. According to this standard, OOK must be employed for low data rate applications. OOK is a special case of binary amplitude modulation using two voltage levels, where the second amplitude is null. It maps bit "0" to "0 volt" and bit "1" to "A volt", A being the amplitude of the OOK signal. The OOK signal will be used as a baseband signal to control the LEDs. The problem of flickering and dimming will rise when OOK is used in VLC: Since the LEDs are powered using a squared wave corresponding to the OOK signal, at very low bit frequency, the human eyes can detect the flickering. It is the important to produce data at a frequency greater than 200Hz. In the case of consecutive zeros, the lighting system will challenge a dimming situation. In this case compensation is needed, this could be done by varying the width of the pulses controlling the LEDs.

C. Visible Light Communication Module Implementation

The circuit used to convey the information through the VLC channel is shown on Figure 2. It shows one side a simple VLC transmitter composed of an LED in series with an opto- coupler and the control part. The control part uses the incoming data to switch the opto-coupler. Receiver side, we have a photo-detector (PD), together with a transistor. The PD collect the message from the channel and the transistor tries to polish the receive signal to produce a pure square wave.

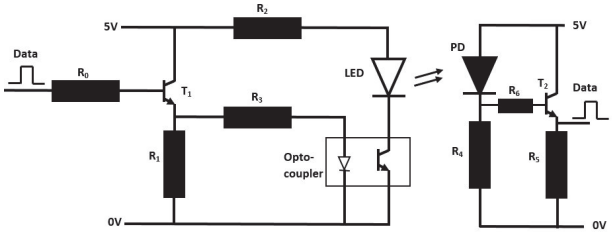

Fig. 2. Schematic diagram of the VLC module implementation.

D. Mamba Narrowband Powerline Communication (NB-PLC) shield

The Mamba NB-PLC shield utilized for the PLC-VLC integration in this work, is a shield that allows the Arduino to get access to this convenient network for data trasnmission and home automation applications. The Mamba shield developed by LinkSprite is pre-built with a Frequency Shift Keying (FSK) modulation scheme and is designed to work under the 110/240V, 50/60Hz supply. The shield is controlled by an

Arduino UNO REV3 board utilizing a simple SPI interface. In other to use the Mamba, two Mamba shield and two Arduino UNO REV3 is required, but for the purpose of this work we use four of both Arduino UNO REV3 and Mamba shield because of our desire to integrate with a VLC system as discussed in the overall system setup in Section III. A 5V, 1A wall adaptor is required to power the Mamba shield for it to work accurately or alternatively, it can be powered via the USB port on the arduino. A Mamba Arduino code written in C++ is used to intialize the module. The code is a simple Universal Asynchronous Receiver/Transmitter (UART) to PLC bridge, as it allows whatever we send to the UART (Transmitter) to be tranmitted on the powerline, and then displayed on the UART (Receiver) at the other end. The following steps are carried out to prepare the module for transmission, while Figure 3 shows a picture of the Mamba NB-PLC shield coupled with the Arduino UNO.

Fig. 3. Picture of Mamba Narrowband powerline communication shield.

1) Install the Arduino-1.0.6-windows IDE version.
2) Install the X-CTU serial terminal software.
3) Plug the Mamba Shield to the computers to be used as a transmitter and Receiver.
4) Open the X-CTU software, the two Arduinos are detected with their precise COM ports.
5) Load the code onto the four Arduino UNOs via the Arduino-1.0.6-windows IDE by selecting the right COM ports.
6) The LED on the shield turns green, an indication that the PLC chip has been initialized and is ready.

E. Semi-Hidden Markov Model

A Fritchman model also regarded as a Semi-Hidden Markov model is used for both the First and Second-order Semi-Hidden Markov modeling in this work. The choice of Fritchman model is based on the fact that it typifies the long bursty error nature of the PLC channel. Fritchman [7], characterized binary communication channel utilizing functions of finite-state Markov chain (FSMC). He proposed the grouping of an N-state model into two major partitions namely an error-free state (good states) and an error state (bad states). A good state is synonymous to an error-free transmission and denoted as "0", while a bad state depicts an occurrence of transmission error, which is denoted by a "1" as shown in Figure 4. For modeling of the burst error PLC-VLC system in this work, a three state model is proposed with two good states and one bad state. Figure 4 shows the Markov chain representation of the Fritchman model.

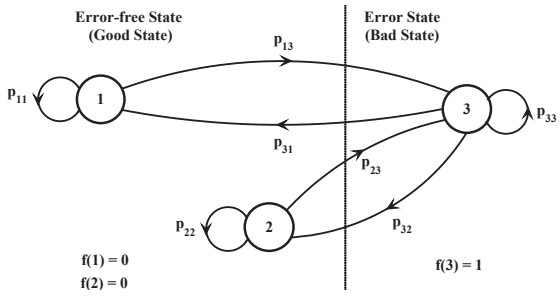

Fig. 4. A Semi-Hidden Markov model (Fritchman model).

F. A First and Second-Order Semi-Hidden Markov Model

Figure 5 shows a First-Order hidden Markov model structure. A First-Order Markov chain model, is one for which the probability of an observation at a particular time t is dependent only on the immediate preceding one. For example, in Figure 5, a current state say S_3 at time t depends on previous state S_2 at time $t-1$ and is mathematically represented as $Pr\ [S_t|S_{t-1}] = Pr\ [S_3|S_2]$. The conditional probability of the first-order Markov model takes the form $p_{ij} = Pr\ [S_{t+1} = j|S_t = i]$ which denotes the probability of transitioning from state i at time t to state j at time $t+1$. Hence the first-order transition matrix P for a three state model assumed for the burst error model is a stochastic 3×3 sized matrix whose row sum up to 1 ($\sum_{j=1}^{N} p_{ij} = 1$). The First-Order state transition matrix P_1 is presented in matrix form in Section III-A.

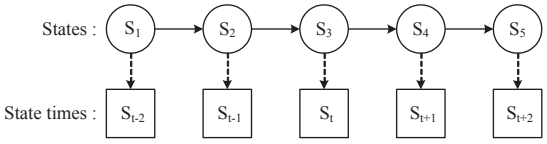

Fig. 5. A First-Order hidden Markov model.

On the other hand, for a second-order Markov chain assumption, probability of an observation at time t depends on two preceding ones. For example, according to Figure 6, current state say S_3 at time t depends on previous states S_2 and S_1 at times $t-1$ and $t-2$ respectively, and is mathematically represented as $Pr\ [S_t|S_{t-1}, S_{t-2}] = Pr\ [S_3|S_2, S_1]$. Hence, the conditional probability of the Second-Order Markov model is denoted as $p_{ijk} = Pr\ [S_{t+2} = k, S_{t+1} = j|S_t = i]$, which denotes the probability of transitioning from state i at time t to state j at time $t+1$ and to state k at time $t+2$. The second-order state transition matrix P_2 is also a a stochastic $3\times3\times3$ sized matrix shown in Section III-A.

Baum welch algorithm [9] is an iterative algorithm designed for re-estimation of the model parameters $\Gamma = (P, B, \pi)$ by training the algorithm with a given error sequence obtained through experimental measurement. Baum welch algorithm has been designed to converge to the maximum likelihood estimator of $\Gamma = (P, B, \pi)$ that maximizes Pr $(O|\Gamma)$ [9].

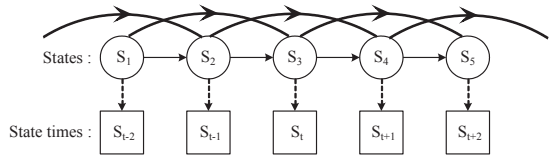

Fig. 6. A Second-Order hidden Markov model.

III. Experimental setup and Methodology

Figure 7 shows the overall architecture of the PLC-VLC integration. A close look at this figure, shows the separation and connection of the PLC main transmitter (Tx) and receiver (Rx) onto different power line outlets. The main Tx is connected to an isolated power line outlet powered through a UPS, while the main Rx is connected to the normal In-House power line topology. This is to ensure that the received data are obtained via the VLC receiver and not from the power line, were they to be connected to the same PLC topology. The dotted arrows shows the data flow direction.

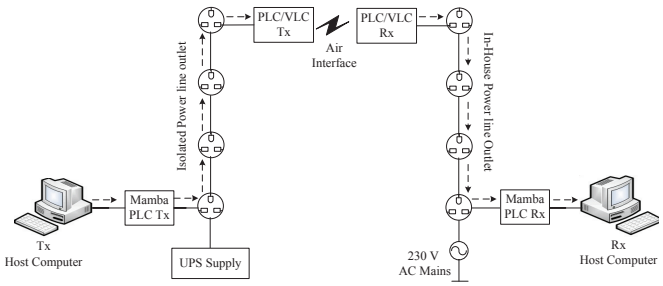

Fig. 7. PLC-VLC integrated architecture showing data flow.

Figure 8 shows a simplified form of the PLC-VLC integration. The Mamba PLC shield is plugged onto the power line and the FSK modulated signal is coupled onto the power line through it. The signal is then captured and demodulated by the PLC receiver. The demodulated signal is routed to the visible light transmitter using the microcontroller. An OOK modulation is then utilized by the VLC transmitter to transmit in a simplex mode. At this stage, the LED converts the received electrical signal into optical signal sent via air interface and received by the VLC receiver through the photo diode which then converts the signal back into electrical form.

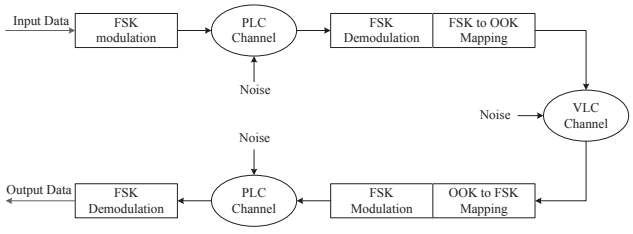

Fig. 8. PLC-VLC Model showing PLC and VLC Interface and modulators.

The system mainly consists of power line and visible light section. PLC employs the infrastructure of electrical power distribution system as communication medium. Power line modem is plugged into the existing power line network and the ASK modulated signal is transmitted through it. This signal is captured by the PLC receiver and it is demodulated. This is routed to the visible light section using microcontroller. FSK modulation is used in VLC and the communication is simplex. Here LED will convert the electrical signal into optical signal which is received using a photodiode and convert back into electrical signal and sends it to the PLC module, which modulates the signal using FSK. The modulated signal is then coupled unto the power line network, after which it is demodulated and reconstructed back into the original sent message by the receiving PLC module.

A. Initial model parameters (First and Second-Order)

The Baum-Welch algorithm used to parameterize the SHMM takes the measured error sequence as training data, and the model's initial parameter as input for the re-estimation of the model parameters. The initial model parameters used are stated as follows.

$$\mathbf{P_1} = \begin{bmatrix} 0.75 & 0 & 0.25 \\ 0 & 0.90 & 0.10 \\ 0.1 & 0.1 & 0.8 \end{bmatrix}. \quad \mathbf{P_2} = \begin{bmatrix} 0.85 & 0 & 0.15 \\ 0 & 0.75 & 0.25 \\ 0.15 & 0.10 & 0.75 \\ 0.7 & 0 & 0.3 \\ 0 & 0.8 & 0.2 \\ 0.10 & 0.25 & 0.65 \\ 0.75 & 0 & 0.25 \\ 0 & 0.90 & 0.10 \\ 0.1 & 0.1 & 0.8 \end{bmatrix}.$$

P_1 and P_2 denotes the First and Second-Order state transition probability matrix respectively. Since a Semi-Hidden Markov model is assumed for this work, the output symbol or error probability matrix B (representing the input-to-output symbol transition) takes the form shown as follows.

$$\mathbf{B} = \begin{bmatrix} 1 & 1 & 0 \\ 0 & 0 & 1 \end{bmatrix}.$$

The first two columns typifies the two error-free state (good states), while the last column symbolizes the error-state (bad state). The initial state probability matrix, which denotes a prior or initial probability of being in any of the state is also written as follows. All the element of the prior probability matrix must sum up to one.

$$\pi = [\pi_1 \ \pi_2 \ \pi_3]. = [0.4 \ 0.4 \ 0.2].$$

IV. Results

The First and Second-Order Semi-Hidden Markov modeling results are discussed in this section.

A. Estimated State Transition Matrix

Table I and Table II show the First and Second-Order re-estimated state transition matrix respectively. The re-estimated state transition matrix depicts the transition of the channel from one state to another depending on the input-to-output

symbol probability matrix, which is influenced by the channel status. The model parameters depicts a distribution of the transmission errors as obtained on the channel through measurement. The error distribution are non-uniform as seen from the state transition probabilities values for the First and Second-Order model. Based on the loglikelihood ratio, we can clearly state that the second order models parameters are the most probable parameters that best fits the model.

TABLE I
FIRST-ORDER ESTIMATED STATE TRANSITION MATRIX FOR RESIDENTIAL AND LABORATORY SITE (MORNING, AFTERNOON AND EVENING)

	Residential			Laboratory		
	Morn.	Aftn.	Even.	Morn.	Aftn.	Even.
p_{11}	0.7602	0.7598	0.7595	0.7592	0.7589	0.7586
p_{13}	0.2398	0.2402	0.2405	0.2408	0.2411	0.2414
p_{22}	0.8925	0.8924	0.8924	0.8923	0.8922	0.8925
p_{23}	0.1075	0.1076	0.1076	0.1077	0.1078	0.1075
p_{31}	0.0600	0.0603	0.0599	0.0596	0.0592	0.0594
p_{32}	0.1424	0.1427	0.1420	0.1431	0.1433	0.1435
p_{33}	0.7975	0.7970	0.7981	0.7972	0.7974	0.7971

TABLE II
SECOND-ORDER ESTIMATED STATE TRANSITION MATRIX FOR RESIDENTIAL AND LABORATORY SITE (MORNING, AFTERNOON AND EVENING)

	Residential			Laboratory		
	Morn.	Aftn.	Even.	Morn.	Aftn.	Even.
p_{111}	0.8512	0.8493	0.8510	0.8509	0.8503	0.8511
p_{113}	0.1488	0.1507	0.1490	0.1491	0.1497	0.1489
p_{122}	0.7506	0.7520	0.7504	0.7502	0.7518	0.7516
p_{123}	0.2494	0.2480	0.2496	0.2498	0.2482	0.2484
p_{131}	0.1505	0.1511	0.1508	0.1506	0.1513	0.1509
p_{132}	0.0996	0.0999	0.0998	0.0992	0.0990	0.0997
p_{133}	0.7499	0.7490	0.7494	0.7502	0.7497	0.7494
p_{211}	0.7042	0.7038	0.7040	0.7045	0.7039	0.7047
p_{213}	0.2958	0.2962	0.2960	0.2955	0.2961	0.2953
p_{222}	0.8112	0.8105	0.8109	0.8107	0.8114	0.8116
p_{223}	0.1888	0.1895	0.1891	0.1893	0.1886	0.1884
p_{231}	0.0998	0.1002	0.0996	0.0987	0.1006	0.0999
p_{232}	0.2415	0.2408	0.2412	0.2416	0.2406	0.2408
p_{233}	0.6587	0.6590	0.6592	0.6597	0.6588	0.6593
p_{311}	0.7504	0.7515	0.7508	0.7511	0.7513	0.7506
p_{313}	0.2496	0.2485	0.2492	0.2489	0.2487	0.2494
p_{322}	0.9096	0.9082	0.9094	0.9888	0.9898	0.9892
p_{323}	0.0904	0.0918	0.0906	0.0112	0.0102	0.0108
p_{331}	0.1005	0.0988	0.1003	0.1000	0.0998	0.0992
p_{332}	0.0988	0.0998	0.0985	0.0991	0.0992	0.0988
p_{333}	0.8007	0.8014	0.8012	0.8009	0.8010	0.8020

B. The Log-likelihood Ratio Plots

Figure 9 and Figure 10 show the loglikelihood ratio plot for the First and Second-Order SHMM respectively. This loglikelihodd ratio is used to acces the fitness of a model i.e it gives a probability of how likely is the data given the parameter estimates. The goal of realizing a model is to obtain parameter values that maximizes the value of the likelihood function. The loglikelihood value is always negative, with higher log-likelihood values (closer to zero) showing and indicating a better fitting model. A comparison of the loglikelihood plot in Figure 9 and Figure 10 show that the Second-Order model produced models with best fit as the higher values are closer to zero compared to the First-Order model.

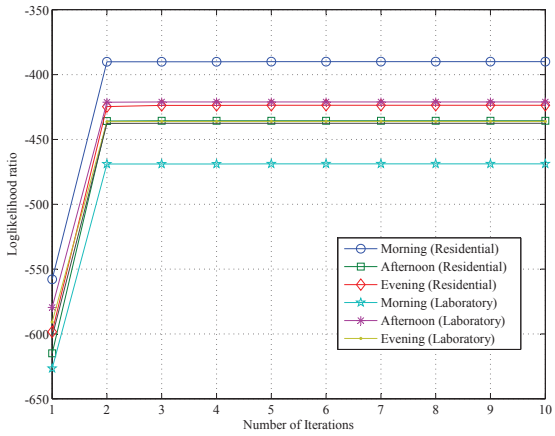

Fig. 9. Loglikelihood ratio plot for the First-Order SHMM.

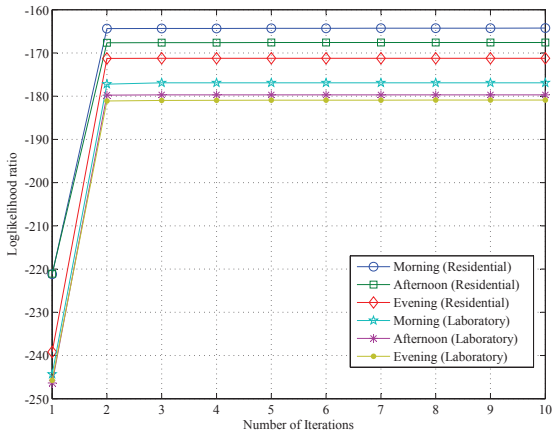

Fig. 10. Loglikelihood ratio plot for the Second-Order SHMM.

C. Error-free run Distribution Plots

Figure 11 and Figure 12 show the error-free run distribution plot. The error-free run plot indicates the runs of m consecutive error-free distribution following an error state. A comparison of the length of intervals m for the First and Second-Order models shows that the Second-Order model has longer runs of error-free runs typifying the measured sequence.

D. Error Probabilities of the models

A comparison between error probabilities between the measured original sequence and the regenerated error sequence

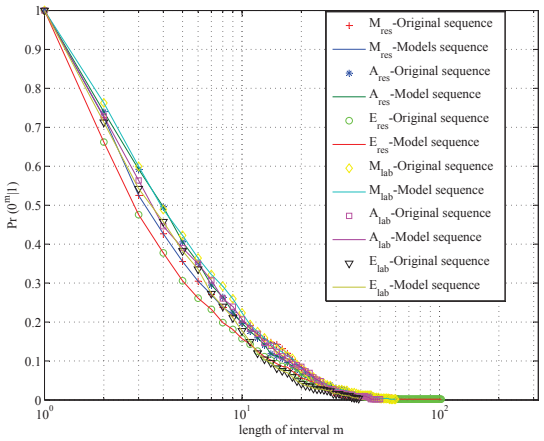

Fig. 11. Error-free run distribution plot for the First-Order SHMM.

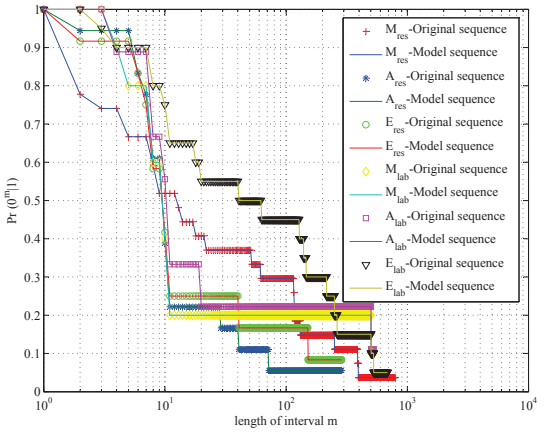

Fig. 12. Error-free run distribution plot for the Second-Order SHMM.

(model) from Tables III shows that the probabilities are in close agreement, in other words there is a close correlation between the error probabilities, hence, validating the model. Similarly, a close look at the Table IV, shows that for the Second-Order Semi-Hidden Markov model, there is close agreement between the original sequence and the model sequence. From Tables III and Table IV, it can be deduced, that the Second-Order model is more accurate with respect to having a more accurate close correlation between the error probabilities of the original error sequence and that of the regenerated error sequence (the model), thus validating the model and corroborating the point that higher order model such as the Second-Order models are better models than the First-Order ones.

V. Conclusion

An implementation of a low cost, low complexity FSK-OOK In-House PLC and VLC Integration utilizing Mamba power line communication shield has been presented. A comparison of the First and Second-Order Semi-Markov Modeling of the burst error that occurs on the overall system has also been done. According to the results obtained, the Second-order Semi-Hidden Markov model yielded a better and more precise model than the First-Order model, which is what we expected according to literature. The resulting statistical models furnishes us with information about the distribution of the burst errors. The Second-Order model, which is a more accurate model will be used to facilitate the design and evaluation of forward error correcting codes for burst error mitigation, as well as using it to optimize the overall system performance.

TABLE III
Error probabilities for measured original error sequence (P_e) and model regenerated error sequence ($\bar{P}_e$)- First-Order SHMM

	Residential			Laboratory		
	Morn.	Aftn.	Even.	Morn.	Aftn.	Even.
P_e	0.0588	0.0278	0.0677	0.0434	0.4568	0.0269
$\bar{P}_e$	0.0569	0.0268	0.0657	0.0426	0.4547	0.0258

TABLE IV
Error probabilities for measured original error sequence (P_e) and model regenerated error sequence ($\bar{P}_e$)- Second-Order SHMM

	Residential			Laboratory		
	Morn.	Aftn.	Even.	Morn.	Aftn.	Even.
P_e	0.0433	0.0258	0.0536	0.0422	0.4354	0.0265
$\bar{P}_e$	0.0430	0.0253	0.0532	0.0419	0.4350	0.0262

References

[1] K. Lee, H. Park, and J. R. Barry, "Indoor channel characteristics for visible light communications," *Communications Letters, IEEE*, vol. 15, no. 2, pp. 217–219, 2011.

[2] H. Elgala, R. Mesleh, H. Haas, and B. Pricope, "Ofdm visible light wireless communication based on white leds," in *Vehicular Technology Conference, 2007. VTC2007-Spring. IEEE 65th*. IEEE, 2007, pp. 2185–2189.

[3] S. Nakamura, "Present performance of ingan-based blue/green/yellow leds," in *Photonics West'97*. International Society for Optics and Photonics, 1997, pp. 26–35.

[4] Y. Tanaka, S. Haruyama, and M. Nakagawa, "Wireless optical transmissions with white colored led for wireless home links," in *Personal, Indoor and Mobile Radio Communications, 2000. PIMRC 2000. The 11th IEEE International Symposium on*, vol. 2. IEEE, 2000, pp. 1325–1329.

[5] A. Ndjiongue, H. Ferreira, K. Ouahada, and A. Vinckz, "Low-complexity socpbfsk-ook interface between plc and vlc channels for low data rate transmission applications," in *Power Line Communications and its Applications (ISPLC), 2014 18th IEEE International Symposium on*. IEEE, 2014, pp. 226–231.

[6] S. Rajagopal, R. D. Roberts, and S.-K. Lim, "Ieee 802.15. 7 visible light communication: modulation schemes and dimming support," *Communications Magazine, IEEE*, vol. 50, no. 3, pp. 72–82, 2012.

[7] B. Fritchman, "A binary channel characterization using partitioned markov chains," *IEEE Transactions on Information Theory*, vol. 13, no. 2, pp. 221–227, 1967.

[8] H. Balzter, "Markov chain models for vegetation dynamics," *Ecological Modelling*, vol. 126, no. 2, pp. 139–154, 2000.

[9] W. Tranter, K. Shanmugan, T. Rappaport, and K. Kosbar, *Principles of communication systems simulation with wireless applications*, 1st ed. Prentice Hall Press, 2003.